

Charged Topological Solitons in Zigzag Graphene Nanoribbons

M. P. López-Sancho and Luis Brey

Instituto de Ciencia de Materiales de Madrid, CSIC, 28049 Cantoblanco, Spain

(Dated: November 5, 2018)

Graphene nanoribbons with zigzag terminated edges have a magnetic ground state characterized by edge ferromagnetism and antiferromagnetic inter edge coupling. This broken symmetry state is degenerate in the spin orientation and we show that, associated with this degeneracy, the system has topological solitons. The solitons appear at the interface between degenerate ground states. These solitons are the relevant charge excitations in the system. When charge is added to the nanoribbon, the system energetically prefers to create magnetic domains and accommodate the extra electrons in the interface solitons rather than setting them in the conduction band.

Introduction.- Graphene nanoribbons are very interesting systems not only for their potential applications as connectors in graphene based nano devices, but also by their fundamental physical properties. Many of the exotic properties of graphene have origin on the bipartite character of the honeycomb lattice[1, 2]. Similarly, the magnetic and electric properties of graphene nanoribbons depend dramatically on the atomic termination of the edges[3–7]. The chiral nature of the low energy carriers in graphene makes zigzag nanoribbons to have highly degenerate zero energy states localized at the edges, and this unique property has stimulated the study of magnetic instabilities in these ribbons[8–16].

Zigzag graphene nanoribbons (ZZGN's) are characterized by the number of atoms in the unit cell, N_x , that corresponds to a ribbon width $W = \sqrt{3}N_x a/4$, being a the graphene lattice parameter. The momentum of the electrons along the ribbon, k , is restricted to take values in the one-dimensional Brillouin zone, $0 < k < \frac{2\pi}{a}$. The number of atoms per unit cell determines the number of electronic bands per spin in the Brillouin zone. The low energy conduction band and the high energy valence band are degenerate at the center of the Brillouin zone, and these two bands becomes flatten as the width of the ribbon increases, so that they are practically degenerate at zero energy in the range $\frac{2\pi}{3a} < k < \frac{4\pi}{3a}$. These zero energy states correspond to states localized at the edges of the nanoribbons and because they are located on opposite sublattices of the graphene unit cell they are not coupled by the kinetic energy part of the Hamiltonian.

The degeneracy of the valence and conduction bands produces a sharp peak in the density of states at the Fermi energy that makes the system unstable against broken symmetry ground states. Several *ab initio* density functional based calculations[8, 10, 12], and tight-binding Hamiltonians with long-range[17, 18] or on-site[4] interactions have shown that the electron-electron interaction opens a gap in the electronic structure and induces magnetic order in the ground state. All the theoretical calculations indicate the existence of spin polarization localized near each edge and an antiferromagnetic coupling between opposite edges, see Fig.1(a). This antiferromagnetic coupling between opposite edges satisfies the Lieb's theorem[19, 20]. The exchange interaction between electrons favors the occupancy of electronic states in an edge

with a spin orientation and states with opposite spin in the opposite edge. Zigzag graphene nanoribbons have been obtained by using top-down approximations[21–26], by growing graphene epitaxially on silicon carbide[27–30] and by using on-surface synthesis techniques[31]. Some of these nanoribbons show ballistic transport and have a high performance[29, 30]. In addition, experiments have found proof of magnetic order at zigzag graphene nanoribbons.[25, 31, 32]

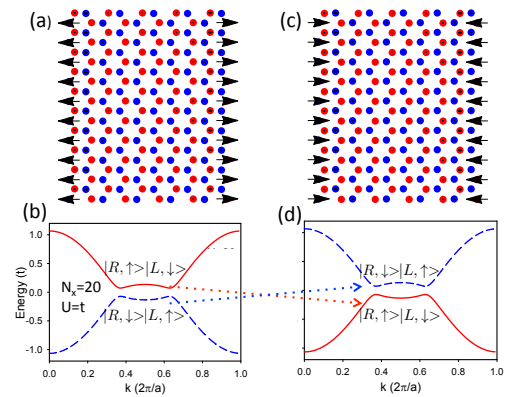


FIG. 1. (a) Schematic picture of the spin polarization of an undoped zigzag nanoribbon. (b) Lowest energy conduction band and highest valence band of a ZZGN with $N=20$, and $U=t$. (c) spin polarization and (d) band structure for the state degenerate with the ground state shown in (a) and (b). In (a) and (c) the spin orientations are rotated to make the figure clearer.

Main conclusions.- By inverting the spin polarization of the full system there is another energy degenerate ground state, see Fig.1(a)-(c). The origin of the degeneracy is the broken symmetry in the spin sector that occurs in the ground state. The band structures of the degenerate ground states are inverted, see Fig.1(b)-(d), and we argue that, when connecting two domains with opposite mass, a symmetry-protected topological state will appear at the interface. Here, the topological defects are soliton-like excitons that carry a charge $\pm e$, with half electron localized at each edge of the nanoribbon. We claim that when doping, the extra charge will accommodate creating do-

main walls between opposite polarized degenerate ground states. Interestingly the topological properties of zigzag graphene nanoribbons are generated by the electron electron interaction and not by spin-orbit[33], orbital[34] or bond ordering[35]. In the following of this letter, we develop these arguments and present numerical results supporting the existence of topological charged excitations in zigzag graphene nanoribbons.

Hamiltonian- In this work we describe the electron-electron interaction in the on-site Hubbard model,

$$H = -t \sum_{\langle i,j \rangle, \sigma} c_{i,\sigma}^{\dagger} c_{j,\sigma} + U \sum_i \hat{n}_{i,\uparrow} \hat{n}_{i,\downarrow}, \quad (1)$$

$$V_{mf} = U \sum_i \left(\sum_{\sigma} (\hat{n}_{i,\sigma} \langle \hat{n}_{i,-\sigma} \rangle - c_{i,-\sigma}^{\dagger} c_{i,\sigma} \langle c_{i,\sigma}^{\dagger} c_{i,-\sigma} \rangle) - \langle n_{i,\uparrow} \rangle \langle n_{i,\downarrow} \rangle + \langle c_{i,\uparrow}^{\dagger} c_{i,\downarrow} \rangle \langle c_{i,\downarrow}^{\dagger} c_{i,\uparrow} \rangle \right) \quad (2)$$

where $\langle \hat{O} \rangle$ means expectation value of the \hat{O} operator. By solving self-consistently the Hamiltonian we obtain the expectation value of charge and spin at every site of the nanoribbon and the band structure. In Fig.1 we plot a typical band structure and magnetic order for the case of an undoped nanoribbon. The bands are spin degenerate and electron electron interaction creates a magnetic order, with ferromagnetic order at the edges that are anti-ferromagnetically coupled. Because graphene has a bipartite lattice atoms in different sublattices have opposite spin polarization.

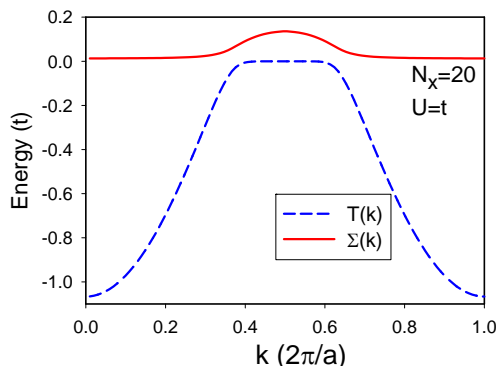


FIG. 2. Selfenergy and tunneling amplitude between states centered in the left and right edges of a nanoribbon as function of the wavevector k . In the calculation we use $N_x=20$ and $U = t$.

2×2 Effective Hamiltonian.- Although the charge density is uniform along and across the nanoribbon, the spin polarization produces spin-dependent electric polarizations[38]. To a great degree of precision the magnetic properties of zigzag graphene nanoribbons can be

here $c_{i,\sigma}^{\dagger}$ creates an electron at site i with spin σ and $\hat{n}_{i,\sigma} = c_{i,\sigma}^{\dagger} c_{i,\sigma}$. In this Hamiltonian hopping exists between nearest neighbor π orbitals with a value $t \approx 2.7\text{eV}$ [1, 2]. The Hubbard model takes into account the short-range part of the Coulomb interaction through the parameter $U > 0$. Experiments[36, 37] give the range of values $U \sim 3.0 - 3.5\text{eV}$. In this work we use a value of $U \sim t$ that yields results in agreement with density functional theory[8, 11]. Exchange interaction is the main ingredient for obtaining magnetic order and therefore Hartree-Fock pairing of the operators is a good approximation for describing magnetic properties of graphene zigzag nanoribbons. The unrestricted Hartree-Fock approximation for the Hubbard term read

described by restricting the Hilbert space to the highest energy valence band, $|k, - \rangle$ and the lowest energy conduction band, $|k, + \rangle$ of the non interacting, $U = 0$, Hamiltonian[38, 39]. The wave functions of these states are even and odd combinations of the π orbitals across the nanoribbon. As the electric and magnetic properties of the nanoribbon are associated with localization of charge at the edges, it is appropriated to use a local base of the form

$$|k, L(R) \rangle = \frac{1}{\sqrt{2}} (|k, + \rangle \pm |k, - \rangle) \quad (3)$$

in this basis the self-consistent Hamiltonian for each spin orientation takes the form,

$$H_{\sigma}(k) = \begin{pmatrix} -\sigma \Sigma(k) & T(k) \\ T(k) & \sigma \Sigma(k) \end{pmatrix} \quad (4)$$

where $\sigma = \pm 1$ for spins pointing up or down respectively, $T(k)$ is the k -dependent hopping between left and right located states and $\Sigma(k)$ is the exchange self energy that has opposite sign for states located on opposite edges or with opposite spin. Both the hopping amplitude and the self energy are real quantities which are obtained by solving self-consistently the Hubbard Hamiltonian. In Fig.2 we plot $T(k)$ and $\Sigma(k)$ for a particular zigzag graphene nanoribbon. From the eigenvectors and eigenvalues of the previous Hamiltonian, the spin-dependent electric dipoles in the transverse direction, \hat{x} , of the nanoribbon, take the form,

$$\mathcal{P}_{\sigma} = e\sigma \sum_k \Sigma(k) \langle k, L|x|k, R \rangle. \quad (5)$$

As commented above the system is not ferroelectric and the sum of the spin-dependent electric dipoles vanishes, $\mathcal{P}_{\uparrow} + \mathcal{P}_{\downarrow} = 0$.

The form of the two Hamiltonians, Eq.4, indicates the degeneracy of the ground state; by reversing the spin orientation of the full system, another degenerate ground state appears, where the spin polarization at the edges and the spin-dependent electric polarization are reversed, see Fig.1. We characterized the two degenerate ground states by $\mathcal{T}=\text{sign}\mathcal{P}_\uparrow$. The index \mathcal{T} shows the spin polarization of the dipole generated in the ribbon by a transversal electric field[38]. The degeneracy of the ground state reflects the broken symmetry of the ground state in the spin sector. Associated with this degeneracy there exist topological excitations, in this case solitons. For each spin orientation, the two degenerate ground states have the bands inverted and therefore there will be two topological protected states, one for each spin orientation, at the interface between domains with opposite \mathcal{T} .

Both Hamiltonians, Eq.4, satisfy the anticommutation relation $\tau_y H_\sigma(k)\tau_y = -H_\sigma(k)$, being τ_y a Pauli matrix. A consequence of this symmetry is that the spectrum of H_σ is electron hole symmetric, any eigenstate $|\psi\rangle$ with energy ϵ has a conjugate state $\tau_y|\psi\rangle$ with energy $-\epsilon$. Because the electron hole symmetry, the topological protected states should be placed at the middle of the gap and get zero energy. Half of the spectral weight of the mid gap state comes from the conduction band and the other from the valence band, therefore when the chemical potential is above (below) zero energy, the soliton carries a charge $-e/2$ ($e/2$)[35, 40]. Considering the two spin orientations, the topological excitation in ZZGN's consists of two $e/2$ charged solitons, and carry a total charge e . The connection between topological defects and electric charge suggests that solitons can be the relevant charge excitation in zigzag graphene nanoribbons. Then whenever adding (subtracting) charge to the system an array of solitons can be formed, creating a solitonic phase. The distance between solitons is the inverse of the density of extra charge per unit length in the ribbon.

Numerical results.- To verify and quantify this proposal, we compute the energy and the electric and magnetic properties of a ZZGN in presence of an extra number of electrons. Because of the electron-hole symmetry existing in the system, the calculations are restricted just to the case of doping with electrons. We consider a periodic structure along the nanoribbon, with a supercell containing N_y repetitions of the minimum unit cell, so that the unit cell contains $N_y \times N_x$ carbon atoms. Because of the use of periodic boundary conditions the solitons in the unit cell always appears by pairs. We add a number n_{extra} of electrons to the unit cell and because of the one dimensional nature of the system the excess of charge is expressed as density of electrons per unit length in the ribbon, $\delta n = n_{extra}/(N_y a)$. By solving self-consistently the Hubbard Hamiltonian in the unrestricted Hartree-Fock approximation, we obtain the energy and the spin and charge spatial distribution in the ribbons as function of the electron density. The solutions converge to the solitonic phase when imposing the initial guess with the

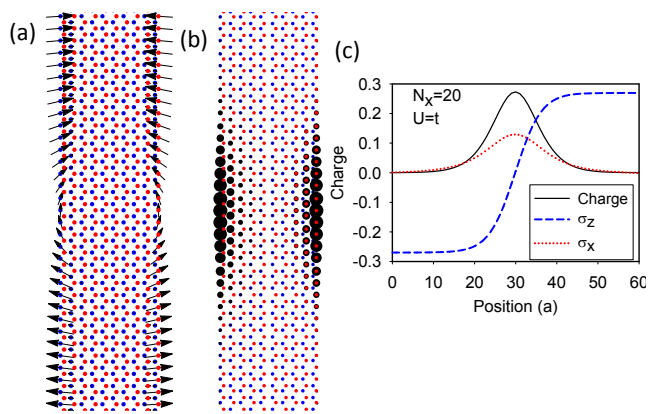


FIG. 3. (a) Local spin polarization and (b) excess of charge near a domain wall separating two degenerate gapped ground states. In (c) we plot the same quantities on the outermost atom in the left edge of the ribbon as function of the position along the ribbon. In the right edge σ_z changes sign, whereas σ_x does not. In (a) the orientation of the spins are rotated to make the figure clearer. In the calculations we use $N_x=20$, $N_y=120$ and $U = t$.

appropriated spin-spatial distribution. In Fig.3 we show the spatial spin polarization (a) and charge distribution (b) for a soliton separating two domains with opposite \mathcal{T} . Crossing the domain wall, the spin polarization in the left edge rotates from pointing in the $+\hat{z}$ direction to pointing in the $-\hat{z}$ direction, acquiring the electron spin polarization a small \hat{x} -component. In the right edge, the spin polarization in the \hat{z} direction has opposite sign, whereas the \hat{x} -component of the spin polarization, in both edges, are parallel.

In order to verify that the solitonic phase is the ground state at low densities we compare its energy with the energies of phases with uniform distribution of charge and spin polarization along the nanoribbon. In particular we compare with uniform phases with ferromagnetic (uni-FM) or antiferromagnetic (uni-AFM) coupling between the edges[41]. Strictly, the spin polarization of the uniform doped phases is not collinear and the edge polarizations are slightly canted with respect the FM and AFM order. In Fig.4 we plot the the total energy difference per unit length between the solitonic and the uni-FM and uni-AFM phases, for a nanoribbon with $N_x=20$. The energy is referred to the energy of the uni-FM phase. From the results shown in this figure, we conclude that the solitonic phase is the ground state of the nanoribbon at densities lower than $\delta n \sim 0.05/a$. At these densities the system prefers to create domains with opposite \mathcal{T} and accommodate the extra carriers at the solitons that appear at the domain walls.

Relation with previous works and discussion. Using density functional theory[42] or tight-binding Hamiltonians[41, 43, 44], previous theoretical works have found that zigzag graphene nanoribbons become ferromagnetic when doped. Using the same Hubbard model

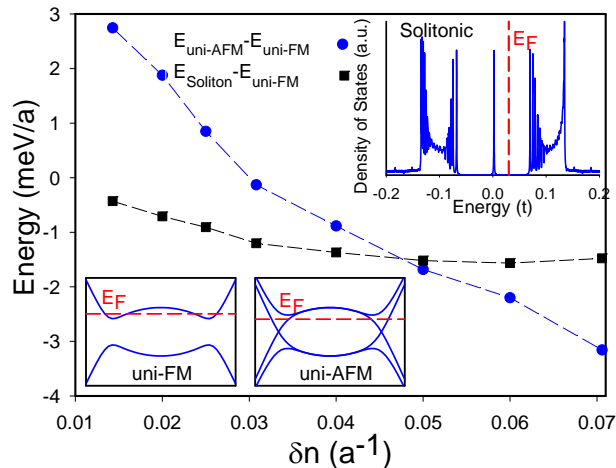


FIG. 4. Energy per unit length of different phases of doped zigzag graphene nanoribbons. The energies are referred to that of the uni-FM phase. At low doping, $\delta n < 0.05/a$ the solitonic phase is the ground state of the system. In the lower panels, we show schematically the band structures of the uniform phases and the position of the Fermi energy. In the inset in the upper part of the figure, we plot the density of states of the solitonic phase. The zero energy peak corresponds to the solitons. The calculations are done with $N_x=20$, $U = t$ and $t=2.7eV$.

than us, Jung and MacDonald[41] find the transition from the uni-FM to the uni-AFM at a density $\delta n \sim 0.03/a$. However, all these calculations do not allow the modulation of the charge and spin along the ribbon, and therefore did not find any clue for the existence of the solitonic phase. The presence of a solitonic phase in zigzag graphene nanoribbons should be detected in transport experiments, as a significant enhancement in the electrical transport in the middle of the energy gap. Also

in the case of solitons trapped by defects or impurities, individual solitons could be visualized by scanning tunneling microscopy experiments. The typical size of the solitons is of some graphene lattice parameters, $\sim 20a$, and their existence would require nanoribbons with magnetic correlation length larger than this size. Recent calculations by Yazyev *et al.*[12] have shown that, at low temperatures, the correlation length in ZZGN's could be as large as 300 at 10K, and this means that solitons can be observed at low temperatures. The calculations presented in this work are done for ribbons with $N_x=20$, we have checked that solitonic phases appear in wider ribbons. The conditions for the appearance of solitons is the existence of an energy gap, and in ZZGN's the gap scales as W^{-1} [39]. The value of the gap increases with the value of the Hubbard interaction U , in our calculations we use a value of $U=t$, that reproduces the gap obtained in density functional calculations. Non local Coulomb interactions can modify the value of U , and recently truly *ab initio* calculations[45, 46] have reported a value of $U \sim 2t$, that makes the magnetic ground state of the ZZGN more stable and, therefore more robust the existence of a solitonic phase .

In summary, we have shown that the low energy charge excitations in doped graphene zigzag nanoribbons are solitons. These solitons appear because of the degeneracy of the magnetic broken symmetry ground state of the ribbon. The two degenerate states have the electronic bands inverted, and when joining two opposite magnetic domains a topological soliton will appear at the interface. The solitons are the low energy charge excitations in the system, and when doping the extra charge will create magnetic domains and will accommodate at the solitons.

Acknowledgments.- M.P.L.-S. acknowledges financial support by the Spanish MINECO Grant No. FIS2014-57432-P, the European Union structural funds and the Comunidad Autónoma de Madrid MAD2D-CM Program (S2013/MIT-3007). LB acknowledges financial support by the Spanish MINECO Grant No. FIS2015-64654-P.

-
- [1] A. H. Castro Neto, F. Guinea, N. M. R. Peres, K. S. Novoselov, and A. K. Geim, *Rev. Mod. Phys.* **81**, 109 (2009).
- [2] M.I.Katsnelson, *Graphene* (Cambridge, 2012).
- [3] K. Nakada, M. Fujita, G. Dresselhaus, and M. S. Dresselhaus, *Phys. Rev. B* **54**, 17954 (1996).
- [4] K. Wakabayashi, M. Fujita, H. Ajiki, and M. Sigrist, *Physical Review B* **59**, 8271 (1999).
- [5] L. Brey and H. A. Fertig, *Physical Review B* **73**, 235411 (2006).
- [6] J. J. Palacios, J. Fernández-Rossier, and L. Brey, *Semiconductor Science and Technology* **25**, 033003 (2010).
- [7] M. Zarea, C. Büsler, and N. Sandler, *Physical Review Letters* **101**, 196804 (2008).
- [8] Y.-W. Son, M. L. Cohen, and S. G. Louie, *Nature* **444**, 347 (2006).
- [9] M. A. H. Vozmediano, M. P. López-Sancho, T. Stauber, and F. Guinea, *Physical Review B* **72**, 155121 (2005).
- [10] L. Pisani, J. A. Chan, B. Montanari, and N. M. Harrison, *Physical Review B* **75**, 064418 (2007).
- [11] J. Fernández-Rossier and J. J. Palacios, *Physical Review Letters* **99**, 177204 (2007).
- [12] O. V. Yazyev and M. I. Katsnelson, *Physical Review Letters* **100**, 047209 (2008).
- [13] O. V. Yazyev, *Reports on Progress in Physics* **73**, 056501 (2010).
- [14] J.-W. Rhim and K. Moon, *Physical Review B* **80**, 155441 (2009).
- [15] H. Santos, L. Chico, and L. Brey, *Physical Review Letters* **103**, 086801 (2009).
- [16] A. D. Güçlü, M. Grabowski, and P. Hawrylak, *Physical Review B* **87**, 035435 (2013).
- [17] J. Jung, *Physical Review B* **83**, 165415 (2011).
- [18] Z. Shi and I. Affleck, *ArXiv e-prints* (2017),

- arXiv:1702.00452 [cond-mat.mes-hall].
- [19] E. H. Lieb, *Physical Review Letters* **62**, 1201 (1989).
- [20] L. Brey, H. A. Fertig, and S. Das Sarma, *Physical Review Letters* **99**, 116802 (2007).
- [21] M. Y. Han, B. Özyilmaz, Y. Zhang, and P. Kim, *Physical Review Letters* **98**, 206805 (2007).
- [22] D. V. Kosynkin, A. L. Higginbotham, A. Sinitskii, J. R. Lomeda, A. Dimiev, B. K. Price, and J. M. Tour, *Nature* **458**, 872 (2009).
- [23] X. Li, X. Wang, L. Zhang, S. Lee, and H. Dai, *Science* **319**, 1229 (2008).
- [24] X. Wang and H. Dai, *Nat Chem* **2**, 661 (2010).
- [25] G. Z. Magda, X. Jin, I. Hagymasi, P. Vancso, Z. Osvath, P. Nemes-Incze, C. Hwang, L. P. Biro, and L. Tapasztó, *Nature* **514**, 608 (2014).
- [26] L. Ma, J. Wang, and F. Ding, *ChemPhysChem* **14**, 47 (2013).
- [27] SprinkleM., RuanM., HuY., HankinsonJ., Rubio-RoyM., ZhangB., WuX., BergerC., and de HeerW. A., *Nat Nano* **5**, 727 (2010).
- [28] J. Hicks, A. Tejada, A. Taleb-Ibrahimi, M. S. Nevius, F. Wang, K. Shepperd, J. Palmer, F. Bertran, P. Le Fevre, J. Kunc, W. A. de Heer, C. Berger, and E. H. Conrad, *Nat Phys* **9**, 49 (2013).
- [29] J. Baringhaus, M. Ruan, F. Edler, A. Tejada, M. Sicot, Taleb-IbrahimiAmina, A.-P. Li, Z. Jiang, E. H. Conrad, C. Berger, C. Tegenkamp, and W. A. de Heer, *Nature* **506**, 349 (2014).
- [30] J. Baringhaus, M. Settnes, J. Aprozanz, S. R. Power, A.-P. Jauho, and C. Tegenkamp, *Physical Review Letters* **116**, 186602 (2016).
- [31] P. Ruffieux, S. Wang, B. Yang, C. Sánchez-Sánchez, J. Liu, T. Dienel, L. Talirz, P. Shinde, C. A. Pignedoli, D. Passerone, T. Dumslaff, X. Feng, K. Müllen, and R. Fasel, *Nature* **531**, 489 (2016).
- [32] C. Tao, L. Jiao, O. V. Yazyev, Y.-C. Chen, J. Feng, X. Zhang, R. B. Capaz, J. M. Tour, A. Zettl, S. G. Louie, H. Dai, and M. F. Crommie, *Nat Phys* **7**, 616 (2011).
- [33] C. L. Kane and E. J. Mele, *Phys. Rev. Lett.* **95**, 226801 (2005).
- [34] L. Brey and P. B. Littlewood, *Physical Review Letters* **95**, 117205 (2005).
- [35] A. J. Heeger, S. Kivelson, J. R. Schrieffer, and W. P. Su, *Reviews of Modern Physics* **60**, 781 (1988).
- [36] S.-i. Kuroda and H. Shirakawa, *Physical Review B* **35**, 9380 (1987).
- [37] H. Thomann, L. K. Dalton, M. Grabowski, and T. C. Clarke, *Physical Review B* **31**, 3141 (1985).
- [38] J. Fernández-Rossier, *Physical Review B* **77**, 075430 (2008).
- [39] J. Jung, T. Pereg-Barnea, and A. H. MacDonald, *Physical Review Letters* **102**, 227205 (2009).
- [40] R. Jackiw and C. Rebbi, *Physical Review D* **13**, 3398 (1976).
- [41] J. Jung and A. H. MacDonald, *Physical Review B* **79**, 235433 (2009).
- [42] K. Sawada, F. Ishii, M. Saito, S. Okada, and T. Kawai, *Nano Letters*, *Nano Letters* **9**, 269 (2009).
- [43] S. Dutta and K. Wakabayashi, *Scientific Reports* **2**, 519 EP (2012).
- [44] S. Li, L. Tian, L. Shi, L. Wen, and T. Ma, *Journal of Physics: Condensed Matter* **28**, 086001 (2016).
- [45] T. O. Wehling, E. Şaşoğlu, C. Friedrich, A. I. Lichtenstein, M. I. Katsnelson, and S. Blügel, *Physical Review Letters* **106**, 236805 (2011).
- [46] M. Schüler, M. Rösner, T. O. Wehling, A. I. Lichtenstein, and M. I. Katsnelson, *Physical Review Letters* **111**, 036601 (2013).